

Heat Exchange in Furnace Side Walls with Embedded Water Cooled Cooling Devices

Gabriel Plascencia
CIITEC -IPN México, D.F.,
México

1. Introduction

Current copper (as well as nickel and lead) smelting and converting are characterized by high intensity and productivity. However, this has led to increasing demands on refractories resulting in possible shortening of the service life of furnace linings. To counteract this, several cooling systems have been designed and implemented in many copper and / or nickel making facilities (Hatch & Wasmund, 1974; Legget & Gray, 1996). The different cooling systems can be grouped according to their ability to remove heat from the hearth of the furnace as shown in Table 1. Cooling systems that are embedded into the furnace refractory lining are able to extract more energy (10 ~ 100 kW/m²) than those acting on the furnace outer shell (~ 1 kW/m²); this main difference is due to the thermal resistance that the insulating refractory lining offers (Legget & Gray, 1996).

System	Location	Heat Flux (kW/m ²)	Applications	Pros	Cons
Plate coolers	Internal	10 - 30	Stack region of iron blast furnaces / flash smelters	High intensity cooling, supports lining	Water leaks, limited by structural considerations
Staves	Internal	20 - 30	Stack region of iron blast furnaces	Applicable in thin wall sections	Limited control, expensive
Internal jackets	Internal	10 - 30	Flash and electric furnaces	Cheaper than plates	Water leaks, uneven cooling
Panels	Internal	> 30	Electric furnaces, Vanyukov bath smelting, Zn fuming	No refractory needed, high heat fluxes	Water leaks, develop mechanical stresses
External jackets	External	5 - 15	Temporary cooling for overheated walls	No need to shut down	Limited heat flux in thick sections
Spray cooling	External	5 - 15	Electric and flash furnace reaction shaft	Cheap, no need to shut down	Corrosion in the outer shell, limited heat flux
Air cooling	External	< 10	Underneath of many furnaces	Cheap, water free	Very low heat fluxes

Table 1. Cooling systems industrially available, after Legget and Gray (Legget & Gray, 1996)

Another factor that affects the difference in the heat flux removal is that the systems that are embedded in the refractory are closer to the furnace's hot face, reducing the effective heat transfer distance, thus increasing the ability to remove heat.

Proper cooling system design is necessary since not every smelter runs in the exactly same manner, as an example, if the side wall heat flux is too low, the refractory may wear back, or if the cooling is highly intense, the excessive cooling may lead to higher heat losses.

Modern smelting processes such as flash, bath or electric furnace, make external cooling unsuitable for their implementation, instead embedded systems are required due to their capacity to extract more heat and thus protect the refractory walls.

Hatch and Wasmund (Hatch & Wasmund, 1974) recognized that refractories are attacked by several mechanisms, such as melting, dissolution by molten metal/slag, chemical reactions between the refractory and the slag. They also acknowledged that refractory spalling may happen as a result of thermal cycling and also tapping and charging operations may promote refractory erosion due to the collision of the charging materials with the lining.

Another problem related to the lining wear is the penetration of molten material into cracks or joints. Thermal cycling not only induces stresses into the lining they also promote the freezing and re-melting of the material deposited on the cracks, enlarging them to a point where leaking of the molten material may produce run outs.

The major operational problems associated with embedded cooling systems are:

- Water leaking through the refractory lining, which in the worst case scenario may result in catastrophic explosions due to the contact of cooling water with the molten metal. It also may happen that the leaked water reacts with the process gas (especially SO_2), resulting in corrosion of the cooling devices, reducing their ability to extract heat.
- Uneven control of the wall heat transfer resulting in either increased refractory wear or heat losses
- Air gaps formed as a result of the thermal cycles experienced by the furnace or due to manufacturing problems of the cooling devices, causing loss of the cooling efficiency.

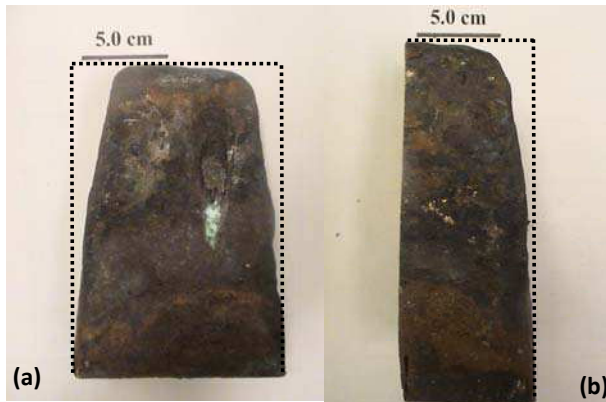


Fig. 1. Hot end of water cooled copper finger after being removed from a flash furnace. (a) Front view, (b) lateral view. The dotted lines represent the original dimensions of the cooler.

Merry et al (Merry et al., 2000) offer similar data on the amount of heat that can be removed with different cooling systems. Notice that in this compilation Merry et al, include finger coolers. These cooling devices are in the mid range in terms of heat removal, they account

for a heat flux capacity of nearly 100 kW/m^2 , which accordingly to Legget and Gray (Legget & Gray, 1996) is equivalent to the energy that can be removed using panel coolers.

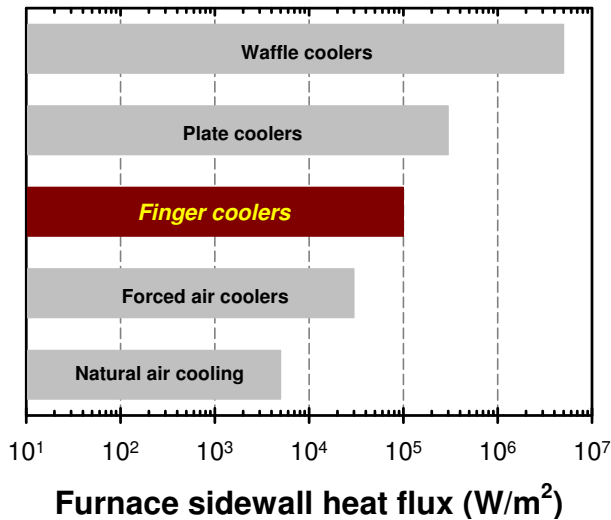


Fig. 2. Furnace side wall heat flux (W/m^2), after Merry et al (Merry et al 2000).

To estimate the actual heat removal capacity of the cooling systems, in this text it is presented the results from some experimental work on laboratory scale finger coolers. These results are then compared with 3-D heat transfer finite element modelling of a real size cooling system. Comparison between experimental data and computations are in very good agreement.

2. High temperature immersion tests

2.1 Materials

The cooling elements used in this work were made of pure copper, copper- 4% wt. aluminium alloy, composite Cu / Cu - 4wt% Al alloy and nickel-plated copper. In each case, high purity copper and aluminium were used. For nickel plating, analytic grade chemicals were used. The design and dimensions of the cooling elements are shown in Figure 3; whereas Figure 4 shows a scheme of the composite cooler.

The copper coolers were machined to the specified dimensions from copper bars. The elements made of the Cu - 4% Al alloy were formed by pre-melting and alloying, before casting and machining. The alloys were machined to the same dimensions as those of the pure copper elements. The composite coolers were made by casting the Cu-4% Al alloy and then machining them into bottom closed hollow cylinders with wall thickness of 3mm; once machined, pure copper was poured into the alloy cylinders. The copper filled cylinders were then machined to the same dimensions as the other cooling elements. The nickel plated copper elements were prepared by plating nickel onto pure copper coolers previously machined. The electrolyte consisted of nickel chloride (240 g/L) and hydrochloric acid (125 mL/L). Electrolysis was carried out between 25 and 29 °C, with a cathode current density of 9 A/m^2 (Aniekwe & Utigard, 1999; Aniekwe, 2000).

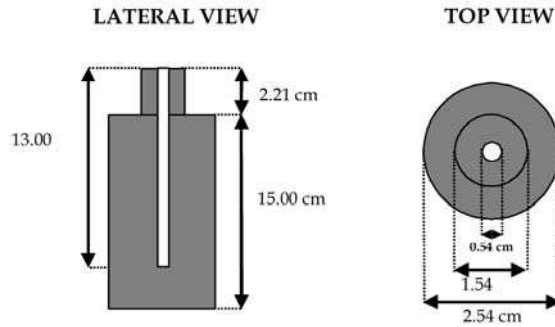


Fig. 3. Schematics of the cooling devices used in this work.

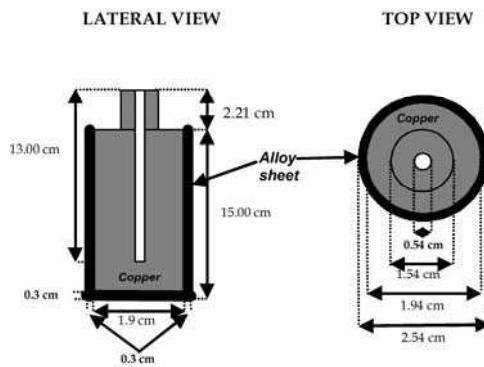


Fig. 4. Schematics of the composite cooling finger.

2.2 Procedures

To remove heat from molten matte or slag, the cooling fingers were screwed to a heat removal device. This device was made of copper and it consisted of a water channel and an opening for a thermocouple. To prevent oxidation of this device, it was covered with boron nitride and fibre glass insulation cloth. Thermocouples were also inserted at the water inlet and outlet respectively.

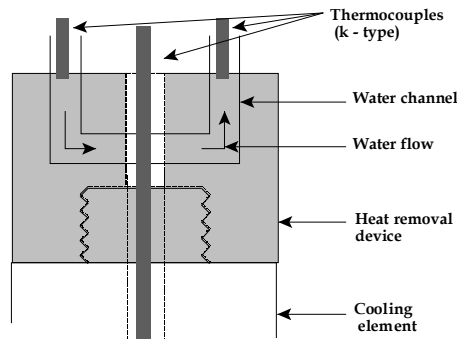


Fig. 5. Schematics of the heat removal device attached to a cooling finger

Immersion tests were carried out in an electric furnace. The cooling fingers were dipped into pre-melted copper matte or slag, both provided by the Xtrata Technology Centre. The tests in mattes were carried out at 1150 °C, while the tests in slags were carried out at 1250 °C. Every test in the matte lasted 1.5 hrs, while those in the slag 2.5 hrs. After these times there was no significant change in any of the temperatures, indicating that steady state had been reached.

The various temperatures were recorded continuously by a data acquisition system. Five k-type thermocouples were used to register the temperature changes in the system. They were located as follows: 1) in the melt, 2) inside the cooler, 3) at the cooler / melt interface (cooler tip), 4) at the water inlet and 5) at the water outlet. Data began to be collected 10 minutes before every immersion test in order to ensure uniform melt temperature. The water flow rate was measured both at the inlet and outlet by means of two flow-meters, and controlled by a third flow-meter with a larger scale.

3. Results and discussion

As mentioned, three different types of finger coolers were tested. The purpose was to compare the thermal response and oxidation behaviour of bare copper and protected copper. The copper was protected in two different ways: 1) Alloying it with aluminium and 2) depositing onto its surface a thick layer (~80 nm) of nickel.

Another important feature of these tests that must be emphasized is that they were performed under extreme conditions. The cooling elements were immersed directly into the molten matte and molten slag with no refractory protection. The reason for performing the tests in this fashion was to evaluate the capacity of protected copper to extract heat from the molten phase and then compare such capacity with that of the un-protected copper. In other words, although the ultimate goal is to protect the refractory lining, in this research, the ultimate goal is to evaluate the thermal and oxidation behaviour of the materials that may be used to construct the cooling systems.

After every test, the cooling element was removed and cut for optical and microscopical examination. Also, X-ray diffraction was carried out on tarnishing products that were peeled off the cooler surface after the immersion test.

3.1 Immersion in a copper matte

The different cooling elements were tested in a Xtrata copper matte (68 wt% Cu) at 1150 °C ± 10 °C. Some of the cooling elements were pre-oxidized in air at 400 °C for 72 hrs in order to estimate the effect of an oxide layer on the cooling efficiency. Such tests are important because it is expected that an oxide layer may form on the cooling devices after being embedded within the refractory lining.

Figure 6 shows typical experimental curves. After approximately 11 minutes into the test, the different temperatures did not change significantly, indicating that steady state was reached. Once steady state was reached, it was possible to estimate the heat flux through the cooling element. The heat flux (q/A) was calculated using the following equation:

$$\frac{q}{A} = \rho_W \times Q_W \times C_{pW} \times \Delta T_W \quad (1)$$

Where A is the area of the cooler that is actually immersed in the molten material (m^2), ρ_W is the density of water (kg/m^3), Q_W is the volumetric flow of the cooling water (m^3/s), C_{pW} is

the heat capacity of water ($\text{J/kg/}^\circ\text{C}$) and ΔT_w is the temperature difference between the outlet and the inlet of the cooling water ($^\circ\text{C}$).

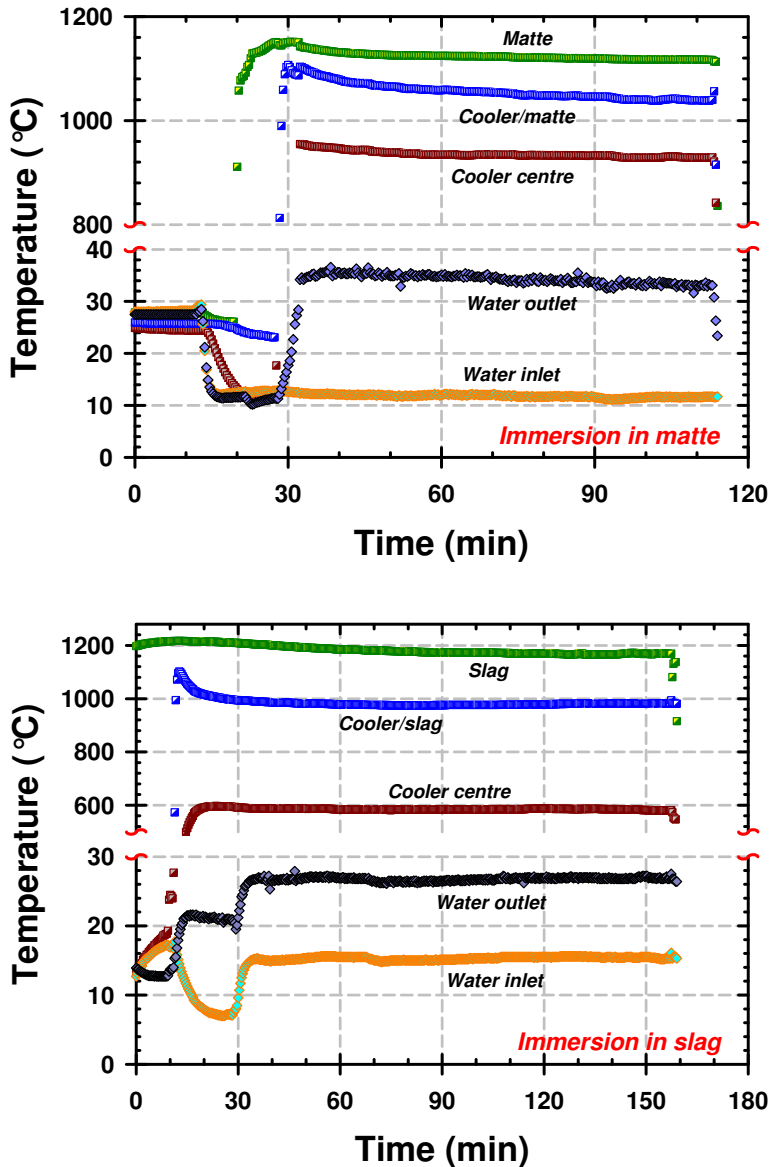


Fig. 6. Typical experimental curves obtained in cooling tests both for matte and slag.

The heat flux shown in Table 2 was estimated using the actual contact area between the cooler and the melt; if only the cross sectional area of the cooler was considered (as it is commonly reported (Hatch & Wasmund, 1974; Merry et al., 2000)), the heat flux through the

copper coolers would have been between 2 and 4 MW/m². The table also shows that the heat flux for the alloy coolers is about 60% lower than that of the copper coolers. Ni plated coolers extract the same energy as the copper coolers.

The tests carried out with cooling fingers made of Cu - 4% Al alloy, registered a mass loss. This mass loss was due to the dissolution of the finger into the matte. This dissolution happens as a result of the inability of this material to extract sufficient heat from the molten matte to promote solidification of a protective shell. However, direct comparison of the actual heat flux extracted with the nominal heat flux for this type of cooling elements in Figure 7.2, reveals that in spite of the dissolution and its poor heat extraction capacity, the alloy cooler still was able to extract up to 5 times more heat from the matte than the maximum recommended in literature (Merry et al., 2000).

On the other hand, the mass increase of coolers made of pure copper or nickel plated copper, showed their ability to solidify matte on them. Table 2 also shows the cooling water temperature change for the different tests carried out. From this table it is clear that the temperature change is very similar for both the copper coolers and the nickel-plated copper coolers, whereas the temperature difference for the alloy coolers is about half of the change registered for the other materials. This decrease of the temperature differential corresponds well with the decrease in thermal conductivity of copper with aluminium alloying. Values reported in the literature (K. Ho & Phelke, 1985; Touloukian & C.Y. Ho, 1970), indicate that the thermal conductivity of the Cu-4% Al alloy is only about 60% of that of pure copper.

After every test, samples of the scales formed on the surface of the coolers during immersion were sent for XRD analysis. Only the copper coolers developed a noticeable external scale, whereas neither the nickel-plated coolers nor the alloy coolers did so. XRD showed that only copper oxides (mainly Cu₂O) were formed, no indication of any sulphide or sulphate or any other possible reaction product was detected.

Cooler	Water flow rate (L/min)	Cooling water temperature change (°C)	Mass change (g)	Heat flux (kW/m ²)	Remarks
4 wt % Al alloy	1.0	16	- 80	350	Not treated
	1.5	13	- 63	427	Not treated
	1.5	15	- 128	492	Pre-oxidized
Ni plated cooler	1.0	26	198	569	Not treated
	1.5	25	150	820	Not treated
	1.5	24	165	788	Pre-oxidized
Bare copper	1.0	28	98	613	Not treated
	1.5	27	158	886	Not treated
	1.5	28	59	919	Pre-oxidized

Table 2. Immersion tests in molten copper matte at 1150 °C

Figure 7 shows the different materials after being immersed in the matte. In the case of the copper cooler, some matte solidified on the bottom end of the cooler. It is also seen that some oxides developed on the cooler surface. In the case of coolers made of the 4% Al alloy, they dissolved after being immersed, with no indication of any solid crust.

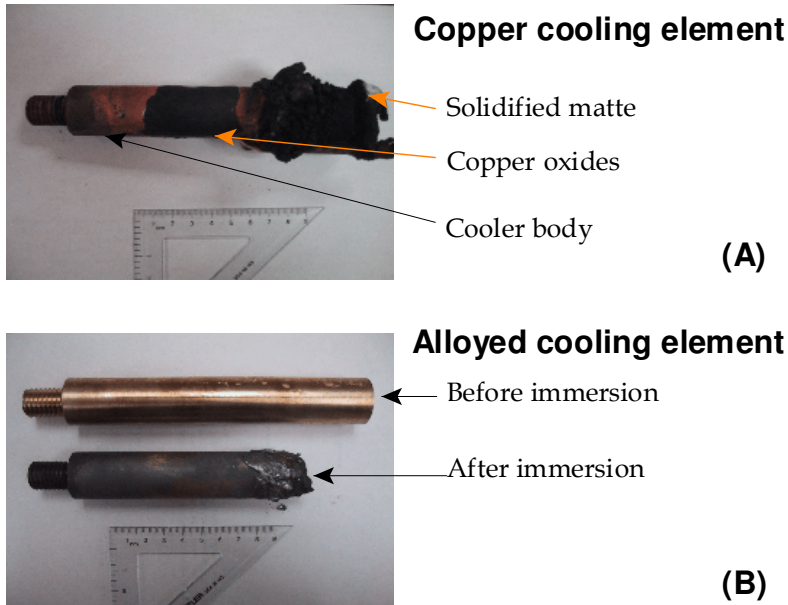


Fig. 7. Cooling elements after being immersed in matte. (A) copper cooler, (B) Cu-Al alloy cooler.

After every immersion test, the bottom end of the cooler was cut and polished for metallographic analysis of the solidified crust. It was found that the crust consisted of a mixture of metallic copper and matte. It seems that some of the copper from the cooling elements began to dissolve into the matte due to the superheat ($66\text{ }^{\circ}\text{C}$ above the melting point of copper) imposed on the cooling element. The copper melting most likely took place at the beginning of the immersion, before the system reached steady state conditions. After this time, the system began to freeze the surrounding matte thus preventing further dissolution of the cooler, retaining the dissolved copper as dispersed droplets through the matte as seen in Figure 8.

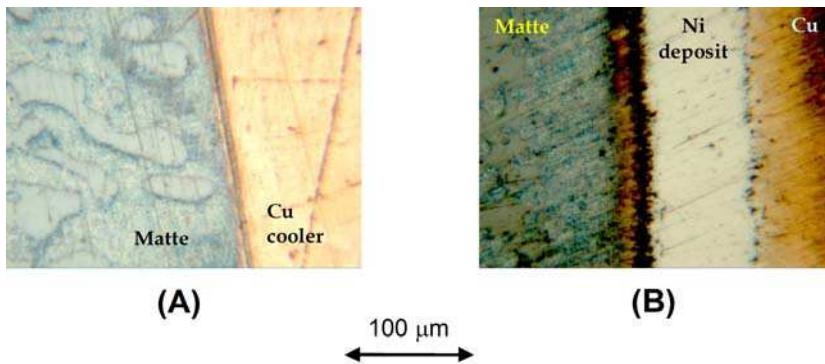


Fig. 8. Metallographs of different cooling elements after immersion in matte. (A) copper cooler, (B) Ni-plated copper cooler.

3.2 Immersion in molten slag

Similar experiments were carried out in a fayalitic (FeSiO_4) based slag; these tests showed that slag is easier to solidify than matte. Figure 6 shows a typical experimental set of curves for the immersion in slag. Such curves are similar to those recorded for the matte immersion tests, the main differences are the lower temperatures as well as the difference in the water temperatures. Although these tests were carried out 100 °C above the matte tests, the cooling elements did not heated up as much as they did when immersed in the matte. At the same time, the difference on temperature of the cooling water slightly decreased for the alloyed coolers, while in the case of the copper and nickel plated coolers the water temperature dropped by nearly 50% of the value recorded in the matte tests. Such decrement clearly indicates that the amount of energy removed from the slag was not as large as the energy removed from the matte. However, the amount of material that can be solidified is very different. Immersion in mattes caused around 150 g of matte to solidify, which represents 5% of the bath weight, whereas the amount of slag that was solidified was about 3.5 kg or 90% of the total bath. This difference can be attributed to the superheat of the different baths. In the case of the matte, the superheat was nearly 120 °C, while in the case of the slag, the superheating was only about 30 °C, thus a small temperature change may induce a more significant solidification rate from the molten slag.

Table 3 summarizes the results from the slag immersion tests and compares them with the results from matte immersion. Notice that the values shown in Table 3 are average values taken once steady state was reached.

Cooler	Molten phase	Hot end temperature (°C)	Cooling water temperature change (°C)	Heat flux (kW/m ²)
4 wt % Al alloy	Slag (1250 °C)	915	9	295
	Matte (1150 °C)	1007	13	427
Ni plated cooler	Slag (1250 °C)	580	11	361
	Matte (1150 °C)	1003	25	804
Bare copper	Slag (1250 °C)	1228	20	574
	Matte (1150 °C)	1102	28	902

Table 3. Immersion in molten slag and matte during 2.5 hrs, with cooling water flow of 1.5 L/min.

3.3 Composite coolers

As mentioned, such elements consisted of a hollow cylinder with the bottom end closed and a wall thickness of 3 mm, made from the Cu - 4 wt% Al alloy. Pure copper was poured into the cylinder cavity and once solidified; the cylinder was machined to the dimensions specified in Figure 4. The motivation for this design was to allow copper to extract heat while being protected from being oxidized by the alloy. Figure 9 shows details of these coolers. Results from immersing these coolers in matte and slag are shown in Table 4.

Cooler	Molten phase	Hot end temperature (°C)	Cooling water temperature change (°C)	Heat flux (kW/m ²)
Composite	Slag (1250 °C)	690	14	335
	Matte (1150 °C)	655	15	418
Bare copper	Slag (1250 °C)	1228	20	574
	Matte (1150 °C)	1102	28	902

Table 4. Comparison of the thermal response between the composite cooler and the copper and alloy coolers (water flow = 1.5 L/min).

As seen in this table, the composite coolers behave in a very similar manner to the coolers made from the alloy, however the amount of energy that they can remove from the molten phase still is 3 times larger than the established design parameters (Hatch & Wasmund, 1974; Merry et al., 2000). Although these cooling elements are not able to extract as much heat as the copper coolers, they offer two main advantages: (1) they are able to keep copper un-attacked by the surrounding atmosphere, extending its service life and (2) They do not suffer any chemical attack from either the matte or the slag. It also must be noticed that by reducing the alloy sheet wall thickness it is possible to improve their capacity to remove energy.

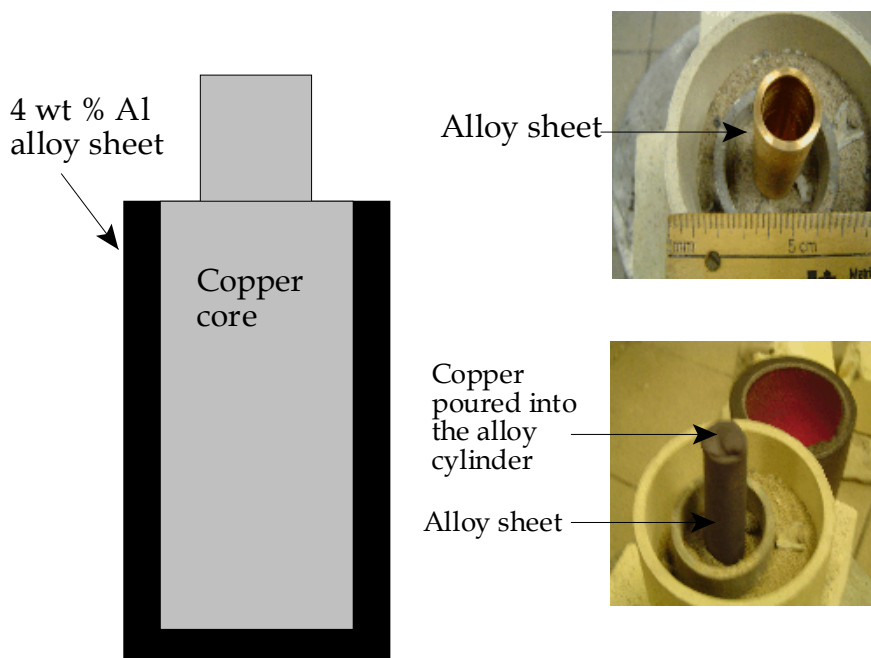


Fig. 9. Details of the pouring of the composite coolers.

4. Mathematical heat transfer modelling

In order to predict the thermal and oxidizing behavior of the cooling elements in an actual furnace, a 3-D mathematical model was set up to estimate the temperature field and the heat flux through the refractory and the cooling elements. The model was set up using the commercial COMSOL Multiphysics software.

4.1 Model set up

The mathematical model was set up based on cooling elements currently in operation at Xtrata's facilities in Sudbury ON (Berryman, 2001). The cooling elements configuration is sketched in Figure 10.

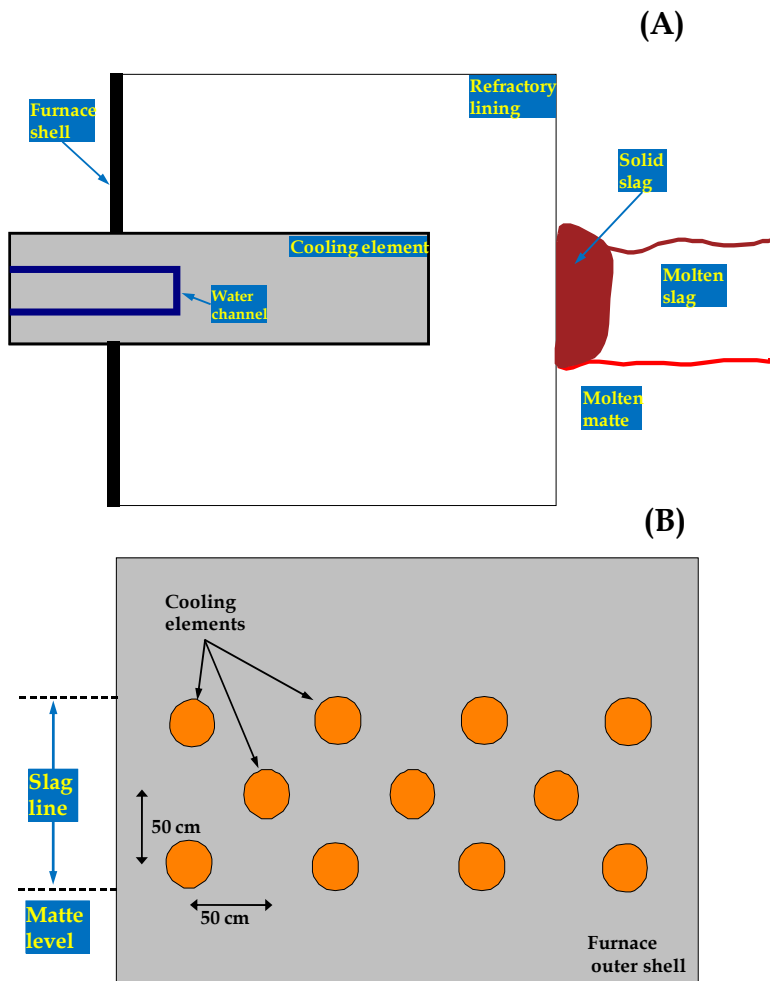


Fig. 10. Schematics of the "finger" cooler cooling device: (A) as it is embedded in the refractory lining. (B) Distribution of the cooling elements alongside the furnace slag line.

In this arrangement, the distance between each cooling element is 50 cm. The cooling elements are long cylinders that are partially embedded into the refractory lining; the unembedded part of the cooler is attached to cooling water through a piping system. The dimensions of each cooler are shown in Table 5.

Dimension	Value (m)
Length	0.79
Diameter	0.15
Water channel length	~0.50
Water channel diameter	0.04

Table 5. Dimensions of the water cooled cooling fingers.

In developing the mathematical modelling it is necessary to evaluate the heat transfer coefficient between the cooling water and the cooling element as well as the heat transfer coefficient between the molten slag and the refractory lining.

Given that the cooling water is forced to run through a circular closed channel, the Dittus-Boelter correlation is the one that better correlates the heat transfer coefficient in turbulent flows (Incropera & DeWitt, 1996). The Dittus-Boelter correlation is expressed as:

$$Nu = \frac{h \times D}{k_{water}} = 0.023 \times Re^{0.8} \times Pr_{water}^{0.3} \quad (2)$$

Where Nu and Re are the Nusselt and Reynolds numbers respectively, Pr_{water} is the Prandtl number for liquid water, k_{water} is the thermal conductivity of water (W/m/K), D is the diameter of the inner channel (m) and h is the heat transfer coefficient between the water and the cooling element (W/m²/K). Equation (2) must satisfy the following conditions:

$$\begin{aligned} 0.7 \leq Pr \leq 160 \\ Re \geq 10^4 \\ \frac{L}{D} \geq 10 \end{aligned} \quad (3)$$

Under the current conditions, the set of conditions (3) are fulfilled, therefore it is possible to use equation (2) to evaluate the heat transfer coefficient. A summary of the estimation of the heat transfer coefficient is shown in Table 6. More detailed data are presented in an earlier work (Plascencia, 2004). In the case of the heat transfer coefficient between the molten phase and the lining, we use a value of h of 1500 W/m²/K as suggested by (Utigard et al., 1994).

u (m/s)	Re	Pr	h (W/m ² /K)
2	86792	5.83	4893.6
4	173583	5.83	8520.2
6	260375	5.83	11784.8
8	347167	5.83	14834.5

Table 6. Heat transfer coefficient for the cooling water as a function of flow velocity

The geometry and the boundary conditions used to run the mathematical model are sketched in Figure 11.

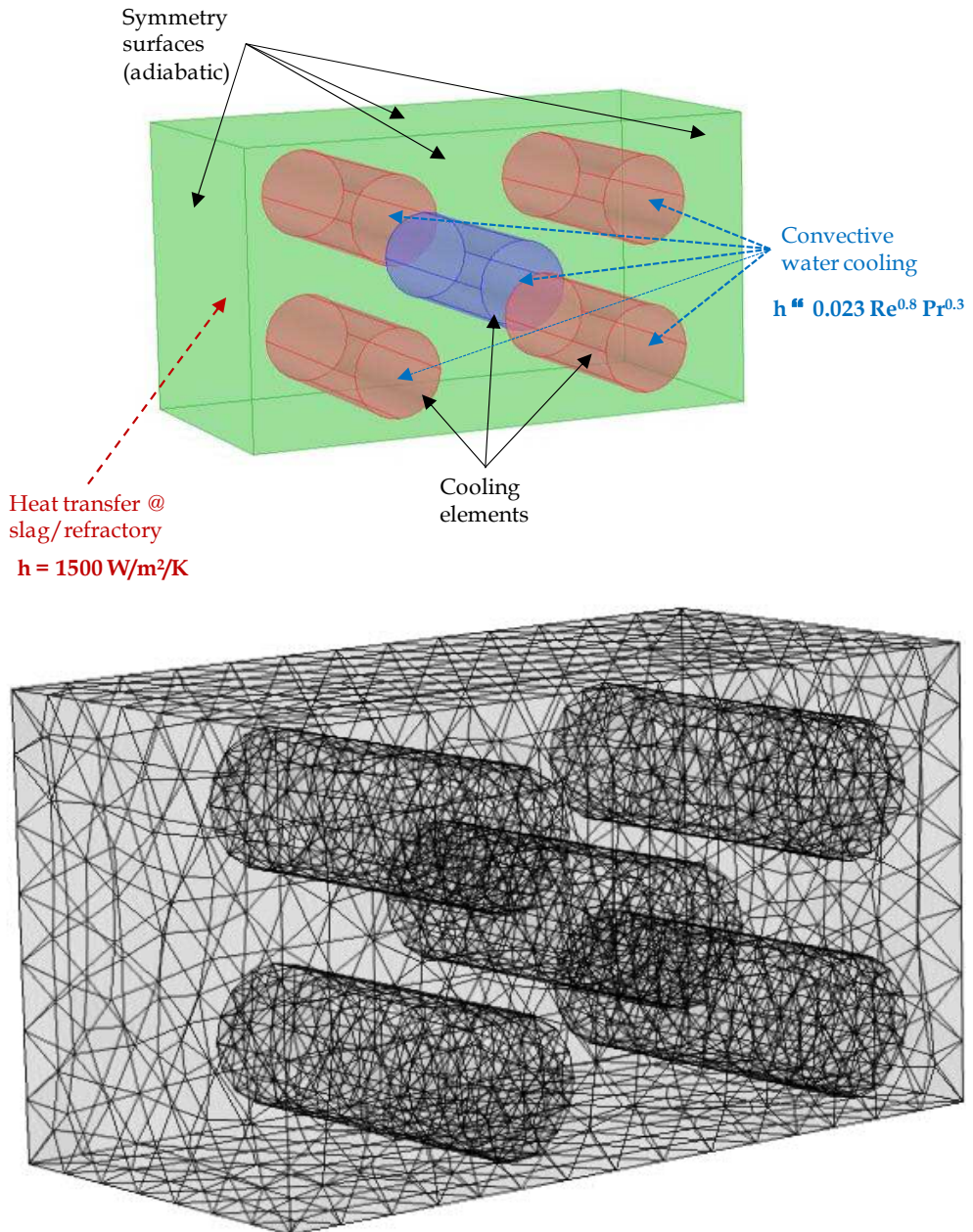


Fig. 11. Boundary conditions and mesh used to run finite element computations.

4.2 Model results

The model was run in order to predict the effect of the refractory thickness in front of the cooler. As expected, as the refractory corrodes away, the hot end temperature of the cooling elements increases. Figure 12 shows results from the modelling.

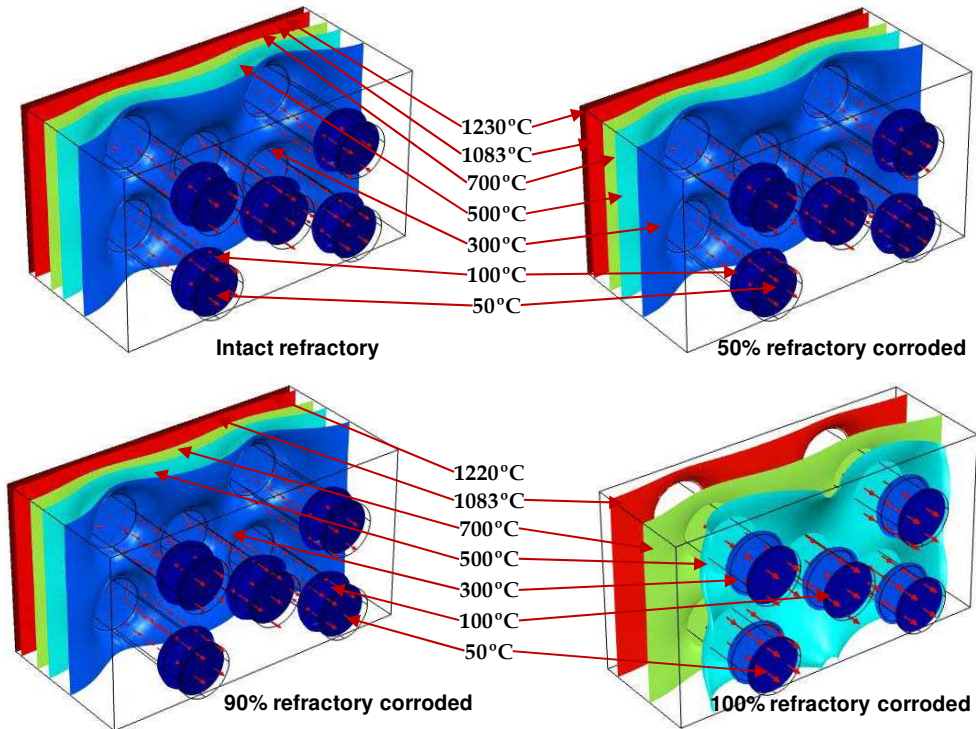


Fig. 12. Computed temperature fields in a 5 cooling elements arrangement.

As the refractory in front of the cooler hot end erodes a shorter path for heat to be extracted is created, additionally, the removal of the refractory decreases the heat transfer resistance so more heat is extracted by the cooler as it is cooled by water. This is shown in Figure 13; this figure indicate that even if the refractory in front of the cooler is completely removed, the cooling water still is able to keep the cooler temperature in the vicinity of 1000 °C, which is below the melting point of copper. This guarantees that the copper from the cooler won't melt down nor dissolve in the slag as it solidifies and in turn, the cooling element will keep its capacity to extract heat from the melt. Unfortunately, reaching the temperature of 1000 °C and under the prevailing process conditions, it is expected that some of the copper would be lost due to high temperature oxidation. The high temperature oxidation may become a problem due to pencilling of the hot end; this means that the ability of the cooling elements to extract heat would be seriously compromised. These calculations are in good agreement with our experimental observations.

It is also evident in Figure 13 that keeping a refractory layer as thin as 2.6 cm (~1 inch) in front of the cooling elements is enough to keep the cooler temperature at a maximum of

about 600 °C. At such temperature (Plascencia 2003), the rate of oxidation of copper is not significant so not much of the metal would be oxidized unless the refractory lining suffers some localized damage or wear. If thicker refractory is kept in front of the coolers, it is expected that the service life of the entire cooling system would be significantly increased. The heat removal capacity of the different systems would remain as designed or even such capacity may be increased.

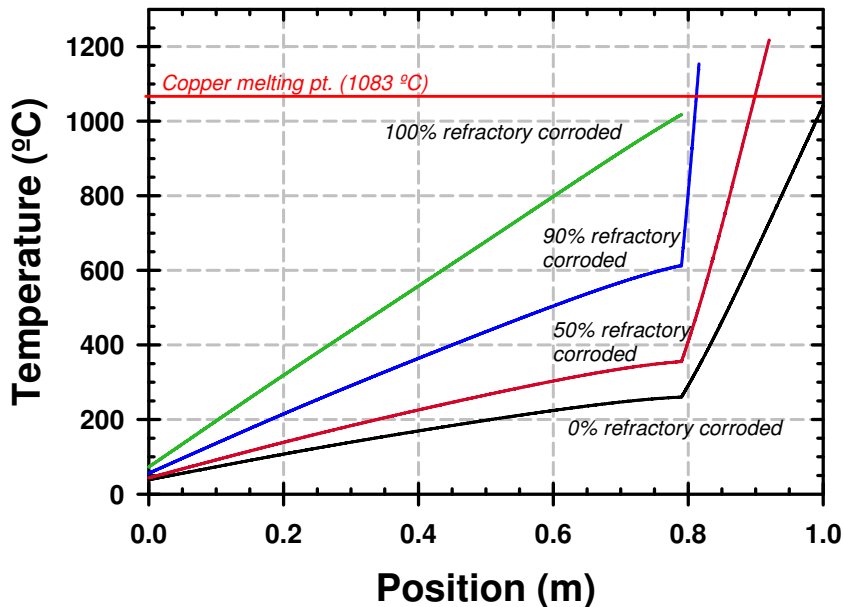


Fig. 13. Temperature profile through the copper fingers and the refractory layer (computed).

The nominal capacity for the fingers cooling systems in terms of the heat flux removed is about 100 kW/m² (see Figure 2). However, as can be seen in Figure 14, that capacity is remarkably surpassed by 5 times in the case of the cooler directly exposed to the molten material. In the case of a cooler with the unworn refractory layer in front of it, the cooler still is able to exceed the nominal capacity by a factor of 1.2. This difference is expected since the exposed cooler has to remove heat directly from the “hot” source with no intermediate thermal resistance, therefore the cooling water passing through the cooler is responsible for the complete elimination of both the sensible and latent heat of solidification.

Table 7 summarizes the main results from our calculations under different set of conditions. In this table T_{cold} represents the temperature at the cold end of the cooler, and T_{hot} represents the temperature at the cooler/refractory interface.

The calculations also reveal that the copper element would lose 6 % of its original length due to dissolution into the molten phase (slag), while the alloy cooler may lose 12 % of its initial length. Direct comparison of the experimental and calculated temperature at the hot end for each cooler are in good agreement, while the calculated and experimental heat fluxes

present a bigger difference. Such difference can be attributed to the material lost due dissolution, since the distance for heat transfer decreases, it results in an increased heat flux. At the same time the difference in the calculated heat fluxes when there is no refractory protection is practically zero; whereas under different lining lengths there are significant differences between the heat fluxes that can be removed using the different coolers.

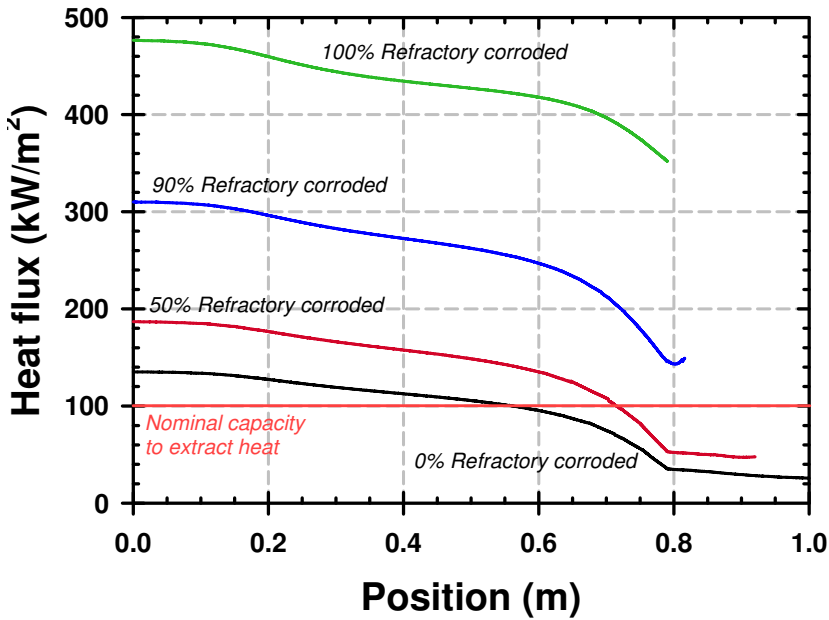


Fig. 14. Heat flux through the copper fingers and the refractory layer (computed).

Material	Refractory in front of the cooler (cm)	T _{hot} Calc. (°C)	T _{hot} Exp. (°C)	Heat flux Calc. (kW/m ²)	Heat flux Exp. (kW/m ²)
Copper	26.0	261	1102	135	574
	13.0	356		187	
	2.6	613		310	
	0.0	1018		476	
Cu - 4wt% Al alloy	26.0	491	1092	94	427
	13.0	794		144	
	2.6	1098		382	
	0.0	1070		733	

Table 7. Comparison of calculated and experimental results

When the refractory lining remains un-attacked, the hot end of the cooling elements does not exceed 500 °C and the rate of oxidation of the tested materials at this temperature is low, thus it would not be expected a failure from the coolers due to air oxidation. However, this

situation is not likely. Since the slags used in copper making have a liquidus temperature around 1150 °C and the actual slag operating temperature varies between 1250 and 1300 °C, a superheat of 150 °C is required to start the solidification of the slag. When we back calculate the superheat from the model results, we found that having the full refractory in front of the cooler would not allow to freeze the slag (superheat = 78 °C) onto the lining surface, indeed the refractory is likely to be eroded. Even after losing 50 % of its original length (superheat = 119 °C), no solid crust would be formed. In order to start the solidification of a protective slag shell, the lining would need to lose around 65 % of its initial length. In such case, the temperature at the hot end of the cooler would be in the vicinity of 700 °C; therefore oxidation of copper may affect the performance of the cooling system.

It also should be noticed that within the furnace, the actual temperature of the slag decreases towards the side walls. This will lead to decreased localized superheats, increased viscosity and decreased fluid flow. All these effects will tend to decrease the heat flux through the side walls, resulting in temperatures of the hot end of the cooler below those calculated above.

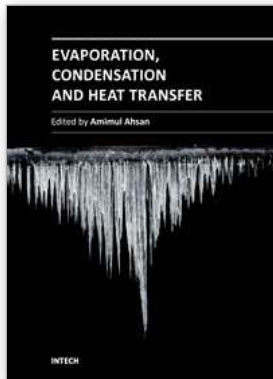
5. Summary

It has been tested different copper based materials as a medium to extract heat from hot furnaces. The effect of high temperature oxidation on the overall performance of the cooling element was also studied. Immersion tests revealed that Cu - Al alloys do not oxidize. However, they are not able to extract heat as effectively as pure copper or nickel-plated copper, resulting in partial melting of the cooling element. These tests also showed that it is easier to solidify slag rather than matte. Numerical calculations may lead to the conclusion that unless the refractory lining is severely damaged, it is unlikely that oxidation of cooling elements would be responsible for the failure of the cooling system. However, the heat flux calculated in un-attacked linings imposes superheats on the slag below that required for freezing a protective shell of slag. Furthermore, in order to start the solidification of the slag onto the lining, for typical slag conditions it is required that the lining reduces its original length by at least 60 %, which may result in the oxidation of coolers made from copper.

6. References

- Aniekwe U V and Utigard T A. 1999, High-temperature oxidation of nickel-plated copper vs pure copper, *Canadian Metallurgical Quarterly*, 38, 4, pp. 277- 281.
- Aniekwe U V. 2000, Protection of Copper Coolers, M.A.Sc. Dissertation, University of Toronto, Toronto, ON, Canada.
- Berryman R. 2001, Private communication, May 2001 Hatch G G, Wasmund B O. 1974, U.S. patent # 3,849,587, Nov. 19, 1974.
- Ho K and Phelke R D. 1985, Metal-Mold interfacial heat transfer, *Metallurgical Transactions B*, 16B, 3, pp. 585 - 594
- Incropera F P and DeWitt D P, *Fundamentals of Heat and Mass Transfer 4th Edition*, John Wiley & sons., New York, U.S.A., 1996.
- Legget A.R., Gray N.B. (1996), Development and application of a novel refractory cooling system. Proceedings of Advances in Refractories for the Metallurgical Industries II, Montréal, QC, Canada, August 1996.

- Merry J., Sarvinis J., Voermann N.(2000), Designing modern furnace cooling systems, *JOM*, 52, 2, pp. 62 - 64.
- Plascencia G, Utigard T A. 2003, Oxidation of copper at different temperatures. Proceedings of the Yazawa International Symposium, San Diego, Cal, USA, February 2003.
- Plascencia G. 2004, High Temperature Oxidation of copper and copper aluminium alloys - Impact on furnace sidewall cooling systems-, Ph. D. Dissertation, University of Toronto, 2004
- Touloukian Y S and Ho C Y Eds., *Thermophysical Properties of Matter*, Vol 1, Thermal Conductivity of Metals and Alloys, Plenum press. New York, U.S.A., 1970.
- Utigard T A, Warczok A and Descaloux P. 1994, The measurement of the heat-transfer coefficient between high-temperature liquids and solid surfaces, *Metallurgical Transactions B*, 25B, 1, pp. 43 - 51.



Evaporation, Condensation and Heat transfer

Edited by Dr. Amimul Ahsan

ISBN 978-953-307-583-9

Hard cover, 582 pages

Publisher InTech

Published online 12, September, 2011

Published in print edition September, 2011

The theoretical analysis and modeling of heat and mass transfer rates produced in evaporation and condensation processes are significant issues in a design of wide range of industrial processes and devices. This book includes 25 advanced and revised contributions, and it covers mainly (1) evaporation and boiling, (2) condensation and cooling, (3) heat transfer and exchanger, and (4) fluid and flow. The readers of this book will appreciate the current issues of modeling on evaporation, water vapor condensation, heat transfer and exchanger, and on fluid flow in different aspects. The approaches would be applicable in various industrial purposes as well. The advanced idea and information described here will be fruitful for the readers to find a sustainable solution in an industrialized society.

How to reference

In order to correctly reference this scholarly work, feel free to copy and paste the following:

Gabriel Plascencia (2011). Heat Exchange in Furnace Side Walls with Embedded Water Cooled Cooling Devices, *Evaporation, Condensation and Heat transfer*, Dr. Amimul Ahsan (Ed.), ISBN: 978-953-307-583-9, InTech, Available from: <http://www.intechopen.com/books/evaporation-condensation-and-heat-transfer/heat-exchange-in-furnace-side-walls-with-embedded-water-cooled-cooling-devices>

INTECH
open science | open minds

InTech Europe

University Campus STeP Ri
Slavka Krautzeka 83/A
51000 Rijeka, Croatia
Phone: +385 (51) 770 447
Fax: +385 (51) 686 166
www.intechopen.com

InTech China

Unit 405, Office Block, Hotel Equatorial Shanghai
No.65, Yan An Road (West), Shanghai, 200040, China
中国上海市延安西路65号上海国际贵都大饭店办公楼405单元
Phone: +86-21-62489820
Fax: +86-21-62489821

© 2011 The Author(s). Licensee IntechOpen. This chapter is distributed under the terms of the [Creative Commons Attribution-NonCommercial-ShareAlike-3.0 License](#), which permits use, distribution and reproduction for non-commercial purposes, provided the original is properly cited and derivative works building on this content are distributed under the same license.